ISSN 1070-3284, Russian Journal of Coordination Chemistry, 2019, Vol. 45, No. 2, pp. 142–153. © Pleiades Publishing, Ltd., 2019.

The Different Effects of Metal Ions on the Synthesis of Macroacyclic Compounds: X-ray Crystal Structure, Theoretical Studies, Antibacterial and Antifungal Activities[1]

M. Rezaeivala[a, *], R. Golbedaghi[b, **], M. Khalili[b], M. Ahmad[c], K. Sayin[d], and F. Chalabian[e]

[a] *Department of Chemical Engineering, Hamedan University of Technology, Hamedan, 65155 Iran*
[b] *Chemistry Department, Payame Noor University, Tehran, 19395-4697 Iran*
[c] *Department of Applied Chemistry, ZHCET, Aligarh Muslim University, Aligarh, India*
[d] *Department of Chemistry, Institute of Science, Cumhuriyet University, TR-58140 Sivas, Turkey*
[e] *Department of Biology, Islamic Azad University, Tehran North Campus, Tehran, Iran*
**e-mail: mrezaeivala@hut.ac.ir*
***e-mail: golbedaghi82@gmail.com*

Received February 21, 2018; Revised September 30, 2018; Accepted October 1, 2018

Abstract—In this work, we have been involved studying the synthesis of some new macroacyclic complexes **I**–**VIII**, so we tried to get propoesed results in all cases but in the case of compound **I**, according to X-ray crystal structure, the product is a protonated Schiff base. By the reaction of a 1 : 1 (metal : ligand) stoichiometry of two known Schiff base ligands, 1,2-bis(2-((2-hydroxy ethylimino)methyl)phenoxy)ethane (H_2L^1) or 1,3-bis(2-((2-hydroxyethylimino)methyl) phenoxy)propane (H_2L^2) and appropriate metal salts in methanol in the case of Ni^{2+}, Cu^{2+} and Co^{2+}, macroacyclic complexes were prepared. When using Mn^{2+} only protonated Schiff base ligands is the final product. All compounds were characterized by microanalysis and IR spectroscopy, whereas compound **I** was also characterized by single crystal X-ray. The X-ray structure of compound **I** showed that both protonated imines are neutralized by two perchlorate ions. Computational calculations of relevant complexes are done by using one of the hybrid density functional theories which are a B3LYP method with 6-31G(d) basis set in a vacuum. Also, the synthesized compounds were screened for their antibacterial activities against nine bacterial strains and showed antibacterial effects. These complexes also showed antifungal effects on two species of Candida.

Keywords: Schiff base ligands, the effect of metal ions, protonated imine, antibacterial, antifungal, crystal structure, theoretical studies

DOI: 10.1134/S1070328419020064

INTRODUCTION

The Schiff bases have been extensively employed in the understanding of molecular processes occurring in biochemistry, antibacterial activities, DNA cleavage, science, catalysis, encapsulation, activation, transport and separation phenomena, hydrometallurgy, etc. [1–3]. A large variety of macrocyclic and macroacyclic ligands have been synthesised to ascertain correctly the role of the different donor atoms, their relative position, the number of the chelating rings formed, the flexibility and the shape of the coordinating moiety on the selective binding of charged or neutral species and on the properties arising from these aggregations [4, 5]. Starting from simple Schiff base ligands, very complex planar or tridimensional cyclic or acyclic systems have been proposed and prepared using self-assembling procedures, recognition processes, template effect, etc. Also, the use of particular complexes as ligands for further complexation has been successfully used [6–8]. The ability of the specific ligand to bind, in appropriate coordination sites, different metal ions is the basic principle for the design of mono and dinucleating or polynucleating complexes. Among the Schiff base ligands, macrocyclic and macroacyclic ligands have an important role to synthesis the new complexes. By searching in literature, only a few examples of protonated imine have been reported [9–13]. Previously, we have reported the synthesis and characterization of some Schiff base complexes [14–18]. Herein, we report the synthesis and characterization of two acyclic Schiff base ligands 1,2-bis(2-((2-hydroxyethylimino)methyl)phenoxy)ethane, H_2L^1 ($n = 2$), 1,3-bis(2-((2-hydroxyethylimino) methyl)-phenoxy)propane, H_2L^2 ($n = 3$) and their

[1] The article is published in the original.

complexes with some of the metal ions (Scheme 1). Quantum chemical calculations have been attractive research field for researchers and scientists [19–21]. The optimized structures of mentioned complexes at electronic ground state are calculated by using computational chemistry method. Some peaks in calculated IR spectra are investigated in detail. Additionally, non-linear optical (NLO) properties of these complexes are examined by using some quantum chemical descriptors which are total static dipole moment (μ), the average linear polarizability (α), the anisotropy of polarizability (Δα), the first hyper polarizability (β), energy of HOMO (E_{HOMO}), energy of LUMO (E_{LUMO}) and energy gap between LUMO and HOMO (E_{GAP}).

Also, the synthesized ligands and complexes were screened for their antibacterial activity and antifungal studies.

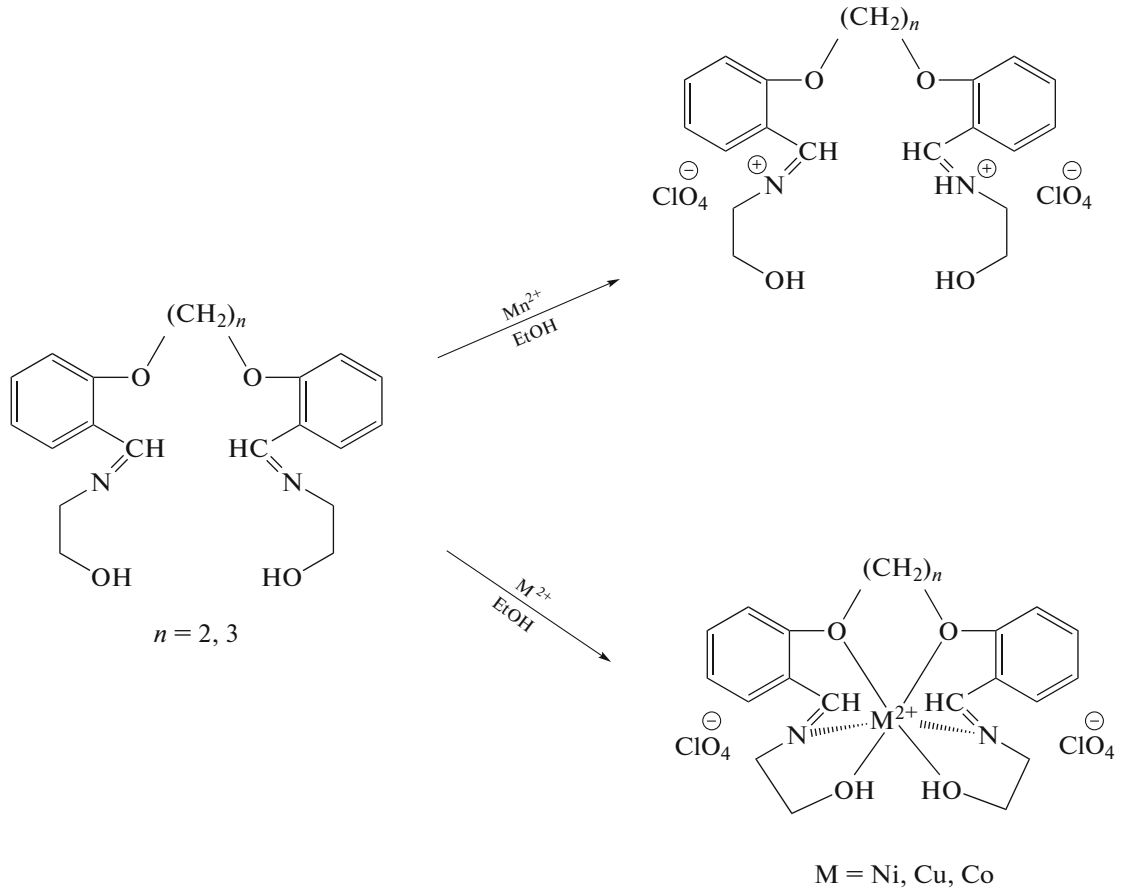

Scheme 1.

EXPERIMENTAL

The various metal salts and ethanol amine were obtained from the Sigma or Merck companies and were used without further purification. IR spectra were measured on a Perkin Elmer FT-IRGX. The Schiff base ligands H_2L^1 and H_2L^2 were prepared according to literature methods [15].

Synthesis of $[(H_2L^1)](ClO_4)_2$ (I). This compound was prepared by 1 : 1 (metal : ligand) stoichiometry of ligand H_2L^1 and $MnCl_2 \cdot 4H_2O$. Ligand H_2L^1 (0.185 g, 0.5 mmol) was dissolved in 10 mL methanol, and the resulting solution was stirred at 30–40°C. The dissolved $MnCl_2 \cdot 4H_2O$ (0.185 g, 0.5 mmol) in MeOH (5 mL) was subsequently added. After refluxing the solution for 24 h, it was filtered while hot, and $NaClO_4$ (1 mmol) was added to the filtrate. The solution was filtered, and the filtrate was reduced to ~10 mL. A crystalline compound was obtained by slow diffusion of Et_2O vapour into this solution. The yield was 29%.

For $C_{20}H_{26}N_2O_{12}Cl_2$			
Anal. calcd., %	C, 43.10	H, 4.70	N, 5.03
Found, %	C, 43.95	H, 4.75	N, 5.02

IR (ν, cm^{-1}): 3417, 1635 ν(C=N Schiff base), 1486 ν(C=C), 1107.9, 625.79 ν(Cl–O).

Synthesis of $[Ni(H_2L^1)](ClO_4)_2$ (II) was carried out by analogous method to **I**. Ligand H_2L^1 (0.370 g, 1 mmol) was solved in 10 mL methanol, and the solution was stirred at 30–40°C. $NiCl_2 \cdot 6H_2O$ (0.236 g, 1 mmol) dissolved in MeOH (5 mL) was subsequently added. The mixture was stirred at 50–60°C for 24 h, then $NaClO_4$ (0.28 g, 2 mmol) was added. The solution was filtered, and the filtrate was reduced to ~10 mL. A crystalline compound was obtained by slow diffusion of Et_2O vapour into this solution. The yield was 20%.

For $C_{20}H_{24}N_2O_{12}Cl_2Ni$

Anal. calcd., %	C, 39.12	H, 3.94	N, 4.56
Found, %	C, 38.95	H, 3.65	N, 4.41

IR (ν, cm^{-1}): 3432 s, 1637.27 ν(C=N Schiff base), 1484.92 ν(C=C), 1061, 624 ν(Cl–O).

Synthesis of $[Co(H_2L^1)](ClO_4)_2$ (III) was carried out by an analogous method to **II** only used $Co(CH_3CO_2)_2 \cdot 6H_2O$. The yield was 23%.

For $C_{20}H_{24}N_2O_{12}Cl_2Co$

Anal. calcd., %	C, 39.11	H, 3.94	N, 4.56
Found, %	C, 38.90	H, 3.55	N, 4.21

IR (ν, cm^{-1}): 3428, 1636, 1486 ν(C=C), 1109, 626 ν(Cl–O).

Synthesis of $[Cu(H_2L^1)](ClO_4)_2$ (IV) was carried out by an analogous method to **II**, only we used $Cu(ClO_4)_2 \cdot 6H_2O$. The yield was 25%.

For $C_{20}H_{24}N_2O_{12}Cl_2Cu$

Anal. calcd., %	C, 38.82	H, 3.91	N, 4.53
Found, %	C, 38.95	H, 3.50	N, 4.10

IR (ν, cm^{-1}): 3442, 1637 ν(C=N Schiff base), 1486 ν(C=C), 1120, 625 ν(Cl–O).

Synthesis of $[H_2L^2](ClO_4)_2$ (V) was carried out by an analogous method to **I** except that we used H_2L^2 instead of H_2L^1. The yield was 67%.

For $C_{21}H_{28}N_2O_{12}Cl_2$

Anal. calcd., %	C, 44.15	H, 4.94	N, 4.90
Found, %	C, 44.25	H, 5.01	N, 4.79

IR (ν, cm^{-1}): 3431.7, 1643.2 ν(C=N Schiff base), 1491.6 ν(C=C), 1106.94, 625.79 ν(Cl–O).

Synthesis of $[Ni(H_2L^2)](ClO_4)_2$ (VI) was carried out by an analogous method to **II** except that we used H_2L^2 instead of H_2L^1. The yield was 67%.

For $C_{21}H_{26}N_2O_{12}Cl_2Ni$

Anal. calcd., %	C, 40.16	H, 4.17	N, 4.46
Found, %	C, 39.90	H, 4.01	N, 4.30

IR (ν, cm^{-1}): 3420, 1652.7 ν(C=N Schiff base), 1487.8 ν(C=C), 1108.9, 625.79 ν(Cl–O).

Synthesis of $[Co(H_2L^2)](ClO_4)_2$ (VII) was carried out by an analogous method to **III** except that we used H_2L^2 instead of H_2L^1. The yield was 75%.

For $C_{21}H_{26}N_2O_{12}Cl_2Co$

Anal.calcd., %	C, 40.14	H, 4.17	N, 4.45
Found, %	C, 39.99	H, 4.02	N, 4.23

IR (ν, cm^{-1}): 3431.7, 1637.7 ν(C=N Schiff base), 1487.9 ν(C=C), 1085.6, 625.79 ν(Cl–O).

Synthesis of $[Cu(H_2L^2)](ClO_4)_2$ (VIII) was carried out by an analogous method to **IV** except that we used H_2L^2 instead of H_2L^1. The yield was 75%.

For $C_{21}H_{26}N_2O_{12}Cl_2Cu$

Anal. calcd., %	C, 39.85	H, 4.14	N, 4.42
Found, %	C, 39.50	H, 3.90	N, 4.10

IR (ν, cm^{-1}): 3412.4, 1637.27 ν(C=N Schiff base), 1488.06 ν(C=C), 1073.19, 623.58 ν(Cl–O).

X-ray structure determination. Single crystal X-ray data of compound **I** was collected at 100 K on a Bruker SMART APEX CCD diffractometer using graphite monochromated MoK_α radiation (λ = 0.71073 Å). The linear absorption coefficients, scattering factors for the atoms, and the anomalous dispersion corrections were taken from the International Tables for X-ray Crystallography [22]. The data integration and reduction were carried out with SAINT [23] software. Empirical absorption correction was applied to the collected reflections with SADABS [24], and the space group was determined using XPREP [25]. The structure was solved by the direct methods using SHELXTL-97 [26] and refined on F^2 by full-matrix least-squares using the SHELXL-97 program [27] package. All non-hydrogen atoms were refined anisotropically. The hydrogen atoms attached to carbon atoms were positioned geometrically and treated as riding atoms using SHELXL default parameters.

Supplementary material for structure **I** has been deposited with the Cambridge Crystallographic Data Centre (no. 1541805; deposit@ccdc.cam.ac.uk or http://www.ccdc.cam.ac.uk/conts/retrieving.html).

Computational method. Computational processes were done with GaussView 5.0.8 [28], Gaussian 09 AM64L-G09RevC.01 package program [29] and ChemBioDraw Ultra Version (13.0.0.3015) [30] programs. Becke-3 parameter-Lee-Yang-Parr (B3LYP) hybrid functional [31, 32] which is one of the density functional theories was selected as computational method for studied complexes and 6-31G(d) was selected as basis set for mentioned complexes. The total μ, α, Δα, β and E_{GAP} are calculated by using Eqs. (1)–(5), respectively:

$$\mu = (\mu_x^2 + \mu_y^2 + \mu_z^2)^{\frac{1}{2}}, \quad (1)$$

$$\alpha = \frac{1}{3}(\alpha_{xx} + \alpha_{yy} + \alpha_{zz}), \quad (2)$$

$$\Delta\alpha = \frac{1}{\sqrt{2}}[(\alpha_{xx} - \alpha_{yy})^2 + (\alpha_{yy} - \alpha_{zz})^2 + (\alpha_{zz} - \alpha_{xx})^2 + 6\alpha_{xz}^2 + 6\alpha_{xy}^2 + 6\alpha_{yz}^2]^{\frac{1}{2}}, \quad (3)$$

$$\beta_0 = [(\beta_{xxx} + \beta_{xyy} + \beta_{xzz})^2 + (\beta_{yyy} + \beta_{yzz} + \beta_{yxx})^2 + (\beta_{zzz} + \beta_{zxx} + \beta_{zyy})^2]^{\frac{1}{2}}, \quad (4)$$

$$E_{GAP} = E_{LUMO} - E_{HOMO}. \quad (5)$$

RESULTS AND DISCUSSION

All compounds **I**–**VIII** were readily synthesized by the reaction of Schiff base ligands, H_2L^1 and H_2L^2 and Mn^{2+}, Ni^{2+}, Co^{2+} or Cu^{2+} metal ions, respectively (Scheme 1). These compounds are quite stable in air and can be stored in a desiccator for long periods of time without decomposition. The resulting compounds were characterized by IR, the elemental analysis in all cases and X-ray diffraction in the case of compound **I**. In this work from the reaction of a 1 : 1 (metal : ligand) stoichiometry H_2L^1 or H_2L^2 and appropriate metal salts in methanol because of the electronic nature of the metal ion and the requirement of preferred geometry of the compounds [33] in the case of Ni^{2+}, Cu^{2+} and Co^{2+}, macroacyclic complexes were prepared but when using Mn^{2+} only protonated Schiff base ligands is the final product. Condensation of all the primary amino group is confirmed by the lack of N–H stretching bands in the IR region (3150–3450 cm^{-1}) and the presence of strong C=N (Schiff base) stretching bands at 1635 and 1643 cm^{-1} for Schiff base ligands H_2L^1 and H_2L^2, respectively. Also, the stretching bands of C=N (imine) compounds have been observed at the range of 1635–1652 cm^{-1}. As it can be seen the bands related to the imine groups in Schiff bases have been shifted in the IR for all compounds, and it can show that the donor atoms in ligands have been coordinated to the metal ions and the complexes have been formed. A broad, intense band at ~1100 cm^{-1} due to ClO_4^- shows no splitting, indicating the absence of coordination of ClO_4^- for all complexes [34, 35]. The NMR studies of Schiff base ligands are completely consistent with their formulation.

Suitable crystal of **I** was obtained by slow diffusion of diethyl ether vapour into a methanol-ethanol solution of the corresponding complexes. A summary of the details of the crystal data, data collection and refinement details are given in Table 1. ORTEP diagram of the molecular structure of **I** is shown in Fig. 1 with the atomic numbering. The X-ray structure of complex **I** shows that both imines are protonated, and the positive charges on the protonated N-atom (iminium ion) are compensated by the negative charges of the perchlorate ions. The 2D supramolecular view of compound **I** is shown in Fig. 2.

The results of antibacterial and antifungal studies have been shown in Table 2. The antibacterial and antifungal effects of components was determined against *B. anthracis* (RTCC 103), *S. aureus* (RTCC 1885), *L. monocytogenes* (RTCC 1885), *S. apyogenes* (RTCC 3024) and *E. faecalis* (RTCC 2121) as gram-positive bacteria and *P. aeruginosa* (RTCC 1547), *K. pneumoniae* (RTCC 1247), *E. aerogenes* (RTCC 1221) and *E. coli* (RTCC 1330) as Gram-negative bacteria. The antifungal activity was determined against two strains of *Candida* including *Candida albicans* (PTCC 5027) and *Candida tropicalis* (PTCC 5028). The results were recorded for each tested compound as the average diameter of inhibition zones of bacterial and fungal growth surrounding the well in millimeters. The compounds exhibited variable antibacterial activity against the above tested bacterial and fungal strains. The results indicated that among all the tested compounds, compound **VIII** showed strong antibacterial activity towards of most bacteria. The significant activity of this compound, especially on Gram-negative bacteria, is important because Gram-negative bacteria are more resistant compared to Gram-positive bacteria. Compounds **IV** and **VII** also have good inhibitory effects on all tested bacteria. It should be noticed that the antibacterial activity of some of these compounds are mainly stronger than standard antibiotics, although some showed the same type of antibacterial activity compared to standards. The results also showed that H_2L^1 and H_2L^2 didn't have any antibacterial activity on all tested bacteria except on *B. anthracis* and *S. apyogenes*. The antifungal results showed that three out of compounds including $[CuH_2L^1](ClO_4)_2$, $[CuH_2L^2](ClO_4)_2$ and $[CoH_2L^1](ClO_4)_2$ showed effective antifungal activities against the fungi specially on *C. tropicalis*.

In vitro activity test was carried out using the growth inhibitory zone (well method) [36, 37]. The antibacterial effects of components was determined against the five Gram-positive bacteria: *Bacillus*

Table 1. Crystallographic data and structure refinement for compound **I**

Parameter	Value
Fw	557.33
Temperature, K	100(2)
Crystal system	Triclinic
Space group	$P\bar{1}$
a, Å	9.8151(11)
b, Å	15.4580(18)
c, Å	17.3485(19)
α, deg	70.109(2)
β, deg	74.021(2)
γ, deg	80.173(2)
V, Å^3	2370.8(5)
Z	4
ρ_{calcd}, g/cm^3	1.561
μ, mm^{-1}	0.343
F(000)	1160
Collected reflections	13036
Independent reflections	8678
GOOF	1.027
Final *R* indices ($I > 2\sigma(I)$)	$R_1 = 0.0706$, $wR_2 = 0.1700$
R indices (all data)	$R_1 = 0.1256$, $wR_2 = 0.2339$

anthracis (RTCC 103), *Staphylococcus aureus* (RTCC 1885), *Listeria monocytogenes* (RTCC 1885), *Entrococcus faecalis* (RTCC 2121) and *Streptococcus apyogenes* (RTCC 3024) and against the four Gram-negative bacteria: *Pseudomonas aeruginosa* (RTCC 1547), *Klebsiella pneumoniae* (RTCC 1247), *Enterobacter aerogenes* (RTCC 1221) and *Escherchia coli* (RTCC 1330) (Table 2).

Microorganisms (obtained from enrichment culture of the microorganisms in 1 mL Muller–Hinton broth incubated at 37°C for 12 h) were cultured on Muller–Hinton agar medium. The inhibitory activity was compared with that of standard antibiotics, such as Gentamycin (10 μg/mL). After drilling wells on the medium using a 6 mm cork borer, 100 μL of solution from different compounds were poured into each well. The plates were incubated at 37°C overnight. The diameter of the inhibition zone was measured as precisely as possible. Each test was carried out in triplicate, and the average was calculated for inhibition zone diameters. A blank containing only dimethysolphoxide showed no inhibition in a preliminary test. The macro dilution broth susceptibility assay was used for the evaluation of minimal inhibitory concentration (MIC) (Table 2). The use of 12 test tubes is required by the macro-dilution method. By including 1 mL Muller–Hinton broth in each test, and then adding 1 mL extract with concentration 100 mg/mL in the first tube, we made a serial dilution of this extract from the first tube to the last tube. Bacterial suspensions were prepared to match the turbidity of 0.5 McFarland turbidity standards. Matching this turbidity provided bacterial inoculums concentration of 1.5 × 108 cfu/mL. Then 1 mL of bacterial suspension was added to each test tube. After incubation at 37°C for 24 h, the last tube was determined as MIG without turbidity.

The typical antifungal activity of Cu(II) and Co(II) complexes on *Candida* spp. (Table 2) shows the significant biological activities of the complexes against examined fungi and also Clotrimazole (300 μg/mL) as the standard. For the evaluation of antifungal activities, two strains of *Candida* obtained from the Persian Type Culture Collection (PTCC), Tehran, Iran, including *Candida albicans* (PTCC 5027) and *Candida tropicalis* (PTCC 5028).

The fungal strains were cultured in Sabouraud dextrose agar (SDA, Merck) under aerobic condition in 28°C for 24–48 h in theincubator. Suspensions of fungi were prepared by picking colonies from appropriately incubated agar cultures into sterile water tube to match a McFarland (barium sulphate standard 0.5) turbidity standard (approximately 1.5 × 108 cfu/mL) (McFarland, 1907).

The agar well method was done as prescribed by NCCLS well. First SDA plates were cultured by the

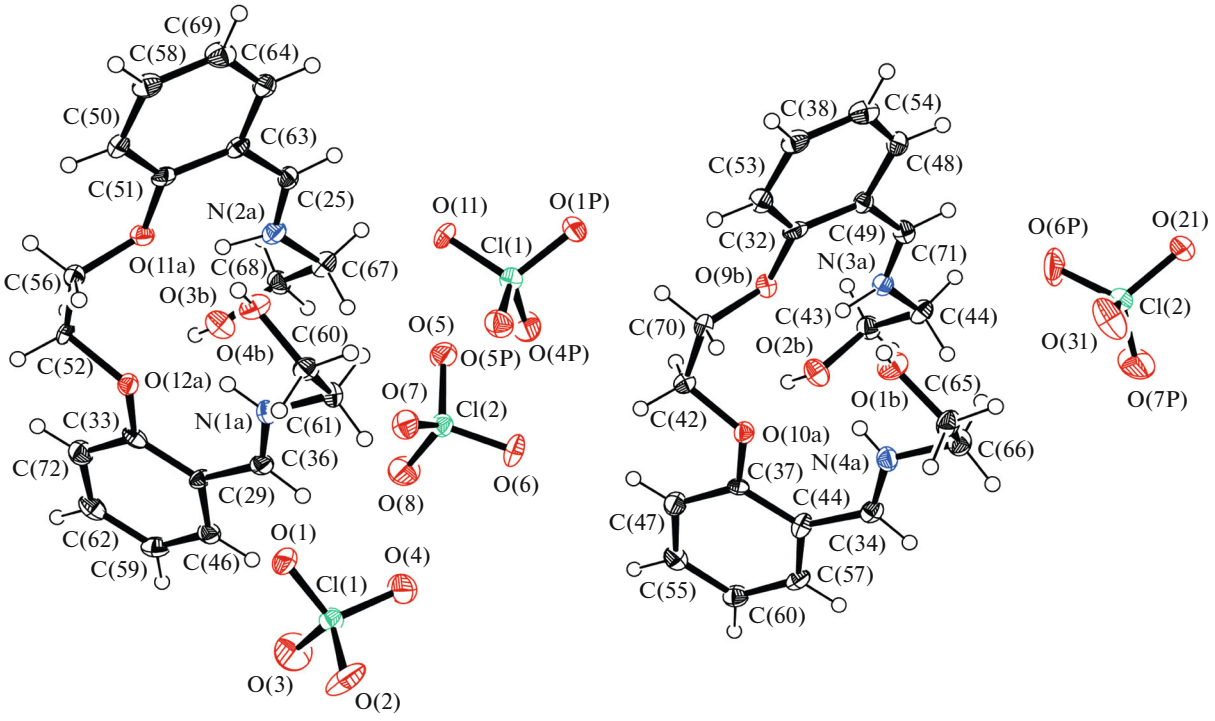

Fig. 1. X-ray crystal structure and ortep view (pictured at 50% probability) of asymmetric compound **I**.

fungal suspension. After drilling wells on the medium by using a 5 mm sterile cork-borer about 2 cm apart, approximately 100 μL of the material suspensions were poured into each well which had filled, respectively, to fullness. After incubation at 28°C for 24–48 h for *Candida* spp., a clear zone around the wells was determined and measured as the zone of inhibition of the complexes on fungal strains growth.

MIC of the extracts was determined according to methods described by CLSI 2006. ZnO suspensions were diluted to concentrations ranging from 100 to 0.78 mg/mL in Sabouraud dextrose broth. To each dilution tubes, 0.1 mL of the fungal suspension was added. Control tubes with no fungal inoculation were simultaneously maintained. Tubes were incubated 6aerobically at 28°C for 24–48 h for *Candida* sp. The lowest concentration of the extract that produced no visible fungal growth (turbidity) was recorded as the MIC (CLSI, 2006). To estimate MIC of the fungi suspensions more precisely and for confirmation of the results, more precise concentration in agar dilution method was used.

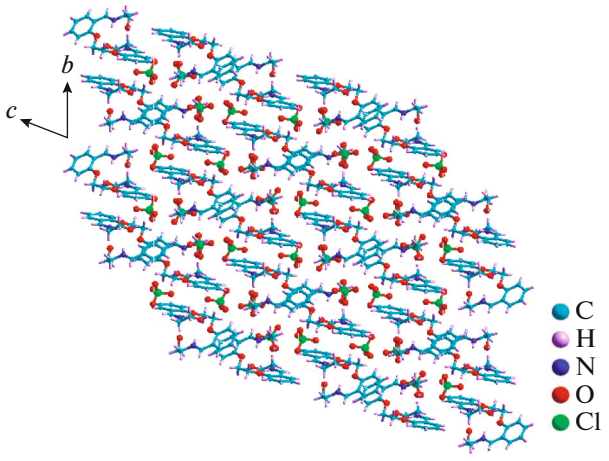

Fig. 2. 2D supramolecular view of compound **I**.

Optimized structures of mentioned compounds are obtained by using B3LYP/6-31G(d) level in a vacuum. Optimized structures of $[M(H_2L^1)]^{2+}$ type complexes and their structural parameters are given in Fig. 3, Table 3, respectively, while optimized structures of $[M(H_2L^2)]^{2+}$ type complexes and their structural parameters are given in Fig. 4, Table 4, respectively.

According to Tables 3, 4, bond lengths of Ni complexes are shorter than those of other complexes. However, related complexes are similar to each other. As for the bond angles and Figs. 3 and 4, electronic structures of mentioned complexesare distorted octahedral.

IR spectra of investigated complexesare calculated at the same level of theory. Some peaks in IR spectra are investigated in detail and listed in Tables 5, 6 for $[M(H_2L^1)]^{2+}$ and $[M(H_2L^2)]^{2+}$, respectively. Calcu-

Table 2. Measured inhibition zone diameter (mm) of the compounds and antibiotics by disc diffusion method, MICs of antibacterial activity of the compounds and antifungal effects on two species of *Candida**

Well method and MIC Bacteria	H_2L^1	H_2L^2	$[CuH_2L^1](ClO_4)_2$	$[CuH_2L^2](ClO_4)_2$	$[CoH_2L^2](ClO_4)_2$	GM 10 μg/mL
B. anthracis RTCC 103 gr+	15 mm 50 mg/mL		10 mm 100 mg/mL	20 mm 25 mg/mL	18 mm 50 mg/mL	25 mm
S. aureus RTCC 1885 gr+			10 mm 100 mg/mL	20 mm 25 mg/mL	10 mm 100 mg/mL	30 mm
L. monocytogenes RTCC 1885 gr+					10 mm 100 mg/mL	25 mm
S. apyogenes RTCC 3024 gr+	15 mm 50 mg/mL		10 mm 100 mg/mL	40 mm 3.12 mg/mL	20 mm 25 mg/mL	20 mm
P. aeruginosa RTCC 1547 g–					15 mm 50 mg/mL	15 mm
K. pneumoniae RTCC 1247 gr–				15 mm 50 mg/ mL	18 mm 50 mg/mL	25 mm
E. aerogenes PTCC 1221 gr–			10 mm 50 mg/mL	15 mm 50 mg/mL	15 mm 50 mg/mL	25 mm
E. faecalis RTCC 2121 gr+			10 mm 100 mg/mL	15 mm 50 mg/mL	15 mm 50 mg/mL	15 mm
E. coli RTCC 1330 gr–			15 mm 50 mg/mL	15 mm 50 mg/mL	15mm 50 mg/mL	10 mm
Fungi						Clotrimazole/mL
Candida albicans PTCC 5027				15 mm 50 mg/mL	15 mm 50 mg/mL	18 mm
Candida tropicalis PTCC 5028				20 mm 25 mg/mL	23 mm 25 mg/mL	20 mm

* Empty cells mean no effect.

lated frequencies are scaled by 0.96 to obtain harmonic frequencies.

As experimentally, vibrational frequencies are very limited while a peak which has the most vibration modes in the band is examined for labelled band as computationally. Therefore, selected frequencies are investigated in detail as computationally. The frequency of OH for $[Cu(H_2L^1)]^{2+}$ has been obtained 1637 and 1556 cm^{-1} in experimentally and computationally, respectively. According to these results calculated frequencies, the frequency of O–H band is calculated in the range of 3160–3600 cm^{-1} and frequency of C=N bond is calculated in the range of 1450–1650 cm^{-1}.

NLO properties can be affected by molecule structure, electromagnetic fields, frequency and these properties are an important properties in providing the key functions of frequency shifting, optical modulation, optical switching, optical logic and optical memory for the technologies in areas such as telecommunications, signal processing and optical interactions. Therefore, NLO is located in the foreground in this study. NLO properties of $[M(H_2L^1)]^{2+}$ and $[M(H_2L^2)]^{2+}$ type complexes are predicted by using some quantum chemical descriptors which are μ, α, Δα, в, E_{HOMO}, E_{LUMO} and E_{GAP}. These descriptors are calculated and given in Table 7 for $[M(H_2L^1)]^{2+}$ and $[M(H_2L^2)]^{2+}$ type complexes.

In computational chemistry, some chemical and electronic properties of similar compounds can be compared with each other. Therefore, NLO properties of $[M(H_2L^1)]^{2+}$ and $[M(H_2L^2)]^{2+}$ type complexes are investigated and compared with each other. In Table 7, quantum chemical descriptors of mentioned complexes and urea are calculated at B3LYP/6-31(d) level. NLO properties can be affected from polarizability, hyperpolarizability and electron mobility. NLO properties increase with increasing the total

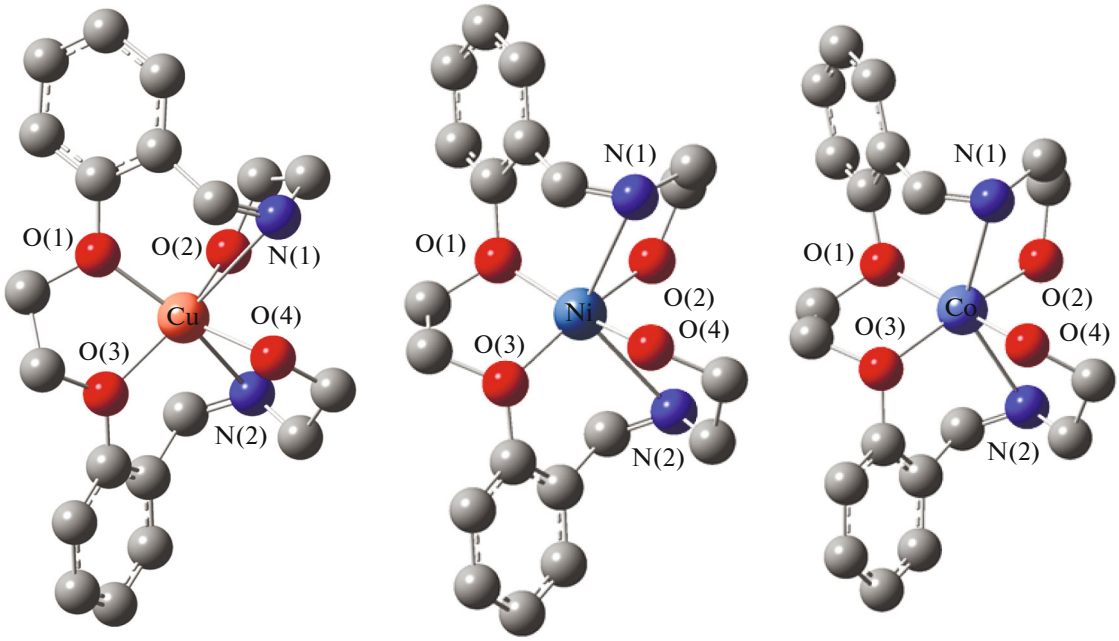

$[Cu(H_2L^1)]^{2+}$ $[Ni(H_2L^1)]^{2+}$ $[Co(H_2L^1)]^{2+}$

Fig. 3. Optimized structures with atomic labelling of mentioned compounds related with (H_2L^1) at B3LYP/ 6-31G(d) level in vacuum and hydrogen atoms are omitted for clarity.

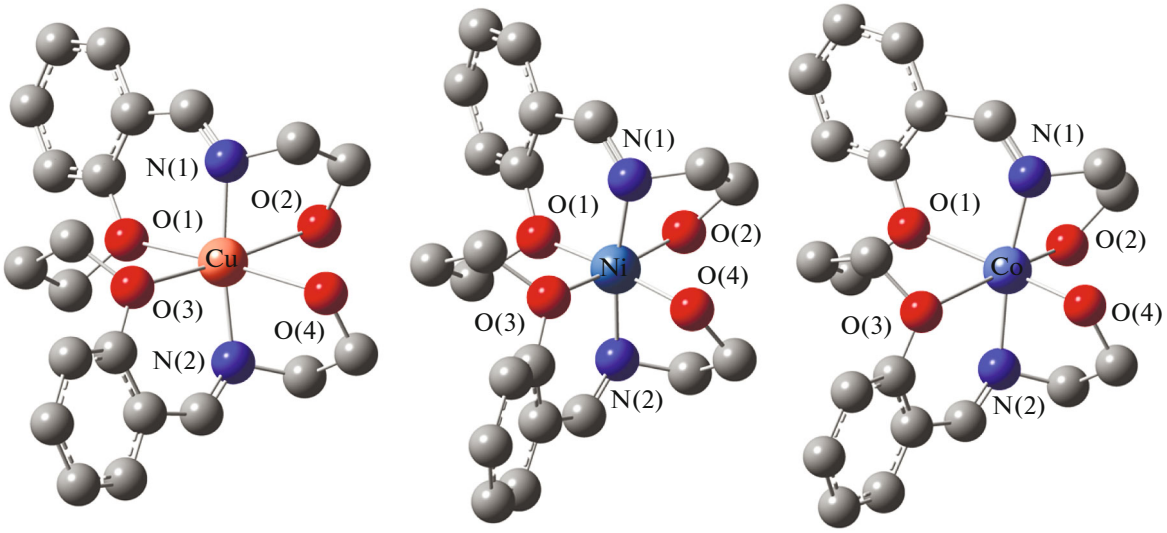

$[Cu(H_2L^2)]^{2+}$ $[Ni(H_2L^2)]^{2+}$ $[Co(H_2L^2)]^{2+}$

Fig. 4. Optimized structures with atomic labeling of mentioned compounds related with (H_2L^2) at B3LYP/ 6-31G(d) level in vacuum and hydrogen atoms are omitted for clarity.

static dipole moment, the average linear polarizability, the anisotropy of polarizability and the first hyper polarizability. Additionally, the mobility of electrons in molecules depends to E_{HOMO}, E_{LUMO} and $E_{LUMO-HOMO}$. The electron mobility is easy with the highest value of HOMO energy, the lowest value of LUMO energy or the smallest values of GAP energy. The average linear polarizability, the anisotropy of

Table 3. Optimized structural parameters of $[M(H_2L^1)]^{2+}$ type complexes at B3LYP/6-31G(d) level in gas phase

Assigment	$[Cu(H_2L^1)]^{2+}$	$[Ni(H_2L^1)]^{2+}$	$[Co(H_2L^1)]^{2+}$
Bond		*d*, Å	
M–O(1)	2.034	1.910	2.036
M–O(2)	1.943	1.886	1.961
M–O(3)	1.999	1.905	2.017
M–O(4)	1.976	1.907	1.955
M–N(1)	2.902	2.787	2.540
M–N(2)	2.661	2.707	2.473
Angle		ω, deg	
O(1)MO(2)	99.3	92.5	95.9
O(1)MO(3)	80.7	85.3	82.7
O(1)MO(4)	136.0	159.7	167.5
O(1)MN(1)	86.8	96.5	96.1
O(1)MN(2)	150.8	127.9	115.4
O(2)MO(3)	142.9	163.1	172.5
O(2)MO(4)	99.2	94.9	91.3
O(2)MN(1)	70.2	71.7	72.3
O(2)MN(2)	70.8	70.9	77.2
O(3)MO(4)	106.4	92.8	91.4
O(3)MN(1)	146.0	125.2	115.2
O(3)MN(2)	91.2	97.3	96.7
O(4)MN(1)	62.9	68.1	76.4
O(4)MN(2)	73.2	72.3	76.1
N(1)MN(2)	113.7	121.7	137.9

polarizability and the first hyper polarizability of mentioned complexes are higher than their ureas value. Therefore, all of them are better than urea in NLO application. According to mentioned descriptors, some ranking are obtained from Table 7 and these ranking are given as follow:

$$\left[Co\left(H_2L^1\right)\right]^{2+} > \left[Cu\left(H_2L^1\right)\right]^{2+} > \left[Ni\left(H_2L^1\right)\right]^{2+} \text{ (for } \mu),$$

$$\left[Co\left(H_2L^2\right)\right]^{2+} > \left[Ni\left(H_2L^2\right)\right]^{2+} > \left[Cu\left(H_2L^2\right)\right]^{2+} \text{ (for } \mu),$$

$$\left[Cu\left(H_2L^1\right)\right]^{2+} > \left[Ni\left(H_2L^1\right)\right]^{2+} > \left[Co\left(H_2L^1\right)\right]^{2+} \text{ (for } \alpha),$$

$$\left[Ni\left(H_2L^2\right)\right]^{2+} > \left[Co\left(H_2L^2\right)\right]^{2+} > \left[Cu\left(H_2L^2\right)\right]^{2+} \text{ (for } \alpha),$$

$$\left[Cu\left(H_2L^1\right)\right]^{2+} > \left[Co\left(H_2L^1\right)\right]^{2+} > \left[Ni\left(H_2L^1\right)\right]^{2+} \text{ (for } \Delta\alpha),$$

$$\left[Ni\left(H_2L^2\right)\right]^{2+} > \left[Co\left(H_2L^2\right)\right]^{2+} > \left[Cu\left(H_2L^2\right)\right]^{2+} \text{ (for } \Delta\alpha),$$

$$\left[Cu\left(H_2L^1\right)\right]^{2+} > \left[Co\left(H_2L^1\right)\right]^{2+} > \left[Ni\left(H_2L^1\right)\right]^{2+} \text{ (for } \beta),$$

$$\left[Ni\left(H_2L^2\right)\right]^{2+} > \left[Co\left(H_2L^2\right)\right]^{2+} > \left[Cu\left(H_2L^2\right)\right]^{2+} \text{ (for } \beta),$$

$$\left[Cu\left(H_2L^1\right)\right]^{2+} > \left[Co\left(H_2L^1\right)\right]^{2+} > \left[Ni\left(H_2L^1\right)\right]^{2+} \text{ (for } E_{HOMO}),$$

Table 4. Optimized structural parameters of $[M(H_2L^2)]^{2+}$ type complexes at B3LYP/6-31G(d) level in gas phase

Assigments	$[Cu(H_2L^2)]^{2+}$	$[Ni(H_2L^2)]^{2+}$	$[Co(H_2L^2)]^{2+}$
Bond	*d*, Å		
M–O(1)	2.344	1.873	2.212
M–O(2)	2.271	1.826	1.878
M–O(3)	2.269	1.864	2.588
M–O(4)	2.295	1.815	1.865
M–N(1)	1.955	1.877	1.964
M–N(2)	1.941	1.887	2.010
Angles	ω, deg		
O(1)MO(2)	104.8	95.5	101.3
O(1)MO(3)	80.1	86.8	77.7
O(1)MO(4)	169.8	171.8	172.4
O(1)MN(1)	83.7	91.7	85.6
O(1)MN(2)	101.4	94.9	103.1
O(2)MO(3)	171.6	172.2	175.6
O(2)MO(4)	68.8	82.4	85.9
O(2)MN(1)	73.2	77.3	78.5
O(2)MN(2)	99.7	95.6	98.5
O(3)MO(4)	107.2	96.3	95.3
O(3)MN(1)	101.0	95.2	105.6
O(3)MN(2)	85.7	91.6	77.7
O(4)MN(1)	101.1	95.6	93.6
O(4)MN(2)	72.7	77.4	78.0
N(1)MN(2)	172.1	170.7	171.3

Table 5. Calculated frequencies and their assignments for each mentioned compounds related with (H_2L^1) at B3LYP/6-31(d) level*

$[Cu(H_2L^1)]^{2+}$		$[Ni(H_2L^1)]^{2+}$		$[Co(H_2L^1)]^{2+}$		$(H_2L^1)^{2+}$	
ν, cm^{-1}	assignment	ν, cm^{-1}	assignment	ν, cm^{-1}	assignment	ν, cm^{-1}	assignment
3315	ν_{OH}	3323	ν_{OH}	3501	ν_{OH}	3384	ν_{OH}
3006	ν_{CH}	3159	ν_{OH}	2977	ν_{CH}	3057	ν_{NH}, ν_{CH}
1648	$\nu_{C=N}$	2966	ν_{CH}	1573	ν_{CH}	1557	$\nu_{C=C}$
1443	α_{CH}	1643	$\nu_{C=N}$	1449	$\nu_{C=N}$	1432	$\nu_{C=C}$, ν_{NH}, ν_{CH}
1308	ω_{OH}	1426	ω_{CH}	1283	ω_{CH}, ω_{OH}	1076	ν_{CN}, $\nu_{C=N}$, $\nu_{C=C}$, ω_{CH}
1191	ω_{CH}, ω_{OH}	1287	ω_{OH}, $\nu_{C=C}$	890	ω_{CH}, ω_{OH}	688	$\omega_{NH,}$ ω_{CH}
1070	$\nu_{C–O}$, $\nu_{C=C}$, ω_{CH}	1190	ω_{OH}	698	ω_{CH}, ω_{OH}	511	ω_{OH}
878	γ_{CH}, γ_{OH}	1058	$\nu_{C–O}$, ω_{CH}	625	$\nu_{C=C}$, ω_{CH}	–	–
724	γ_{OH}	868	γ_{CH}	352	$\nu_{C–O}$, γ_{CH}	–	–

* Vibration modes: ν, stretching; α, scissoring; γ, rocking; ω, wagging.

Table 6. Calculated frequencies and their assignments for each mentioned compounds related with (H_2L^2) at B3LYP/6-31(d) level

$[Cu(H_2L^2)]^{2+}$		$[Ni(H_2L^2)]^{2+}$		$[Co(H_2L^2)]^{2+}$		$(H_2L^2)^{2+}$	
ν, cm^{-1}	assignment	ν, cm^{-1}	assignment	ν, cm^{-1}	assignment	ν, cm^{-1}	assignment
3605	ν_{OH}	3469	ν_{OH}	3580	ν_{OH}	3378	ν_{OH}
2972	ν_{CH}	3071	ν_{CH}	3005	ν_{CH}	3068	ν_{NH}, ν_{CH}
1582	$\nu_{C=N}$	1567	$\nu_{C=N}$, $\nu_{C=C}$	1581	$\nu_{C=N}$, $\nu_{C=C}$	1558	$\nu_{C=C}$, ν_{CH}
1477	α_{CH}, ω_{CH}	1321	$\nu_{C=C}$, ω_{CH}	1472	$\nu_{C=C}$, ω_{CH}	1436	$\nu_{C=C}$, ν_{CH}
1221	ω_{OH}, ω_{CH}	1227	ω_{OH}, $\omega_{CH,}$ ν_{C-C}	1283	–	1092	ν_{CN}, $\nu_{C=N}$, ν_{CO}, ν_{CH}
1010	ν_{C-N}, ν_{C-C}, ν_{CO}	954	γ_{CH}	1107	ν_{CO}, ω_{CH}	733	ν_{CO}, γ_{CH}, ω_{CH}
911	ν_{CO}	884	ν_{CO}, $\nu_{C=C}$, ω_{CH}	969	γ_{CH}	541	ω_{OH}
756	γ_{CH}	627	ν_{C-N}, ν_{C-O}	756	$\nu_{C=C}$, ω_{CH}		

Table 7. Mentioned quantum chemical descriptors for relevant complexes at same level of theory

Complex	μ, Debye	α, Å^3	Δα, Å^3	β, cm^5/esu	E_{HOMO}, a.u.	E_{LUMO}, a.u.	E_{GAP}, a.u.
				$[M(H_2L^1)]^{2+}$			
$[Cu(H_2L^1)]^{2+}$	0.35410	32.12721	69.46762	6.92×10^{-26}	–0.47001	–0.27993	0.19008
$[Ni(H_2L^1)]^{2+}$	0.35350	27.10177	64.34707	6.72×10^{-27}	–0.47466	–0.36688	0.10778
$[Co(H_2L^1)]^{2+}$	0.63236	26.16113	64.46306	2.35×10^{-27}	–0.47391	–0.34660	0.12731
				$[M(H_2L^2)]^{2+}$			
$[Cu(H_2L^2)]^{2+}$	0.76666	30.09961	70.77223	4.59×10^{-27}	–0.45937	–0.29748	0.16189
$[Ni(H_2L^2)]^{2+}$	0.76471	0.873026	31.14942	1.36×10^{-26}	–0.37416	–0.30579	0.06837
$[Co(H_2L^2)]^{2+}$	1.28485	1.341394	30.81895	4.63×10^{-27}	–0.45137	–0.29972	0.15165
Urea	1.81000	1.89786	8.08323	3.81×10^{-28}			

$$\left[Ni\left(H_2L^2\right)\right]^{2+} > \left[Co\left(H_2L^2\right)\right]^{2+} > \left[Cu\left(H_2L^2\right)\right]^{2+} \text{ (for } E_{HOMO}\text{)},$$

$$\left[Ni\left(H_2L^1\right)\right]^{2+} > \left[Co\left(H_2L^1\right)\right]^{2+} > \left[Cu\left(H_2L^1\right)\right]^{2+} \text{ (for } E_{LUMO}\text{)},$$

$$\left[Ni\left(H_2L^2\right)\right]^{2+} > \left[Co\left(H_2L^2\right)\right]^{2+} > \left[Cu\left(H_2L^2\right)\right]^{2+} \text{ (for } E_{LUMO}\text{)},$$

$$\left[Ni\left(H_2L^1\right)\right]^{2+} > \left[Co\left(H_2L^1\right)\right]^{2+} > \left[Cu\left(H_2L^1\right)\right]^{2+} \text{ (for } E_{GAP}\text{)},$$

$$\left[Cu\left(H_2L^1\right)\right]^{2+} > \left[Co\left(H_2L^1\right)\right]^{2+} > \left[Ni\left(H_2L^1\right)\right]^{2+} \text{ (for } E_{GAP}\text{)}.$$

According to these rankings, Cu(II) complexes in $[M(H_2L^1)]^{2+}$ type complexes and Ni(II) complex in $[M(H_2L^2)]^{2+}$ type complexes are mainly the best candidate for NLO application.

ACKNOWLEDGMENTS

We are grateful to the Department of Chemical Engineering, Hamedan University of Technology and Payame Noor University for financial supports. Also,

this research is made possible by TUBITAK ULAKBIM, High Performance and Grid Computing Center (TR-Grid e-Infrastructure).

REFERENCES

1. Alexander, V., *Chem. Rev.*, 1995, vol. 95, p. 273.
2. Fenton, D.E. and Okawa, H., *Chem. Ber.*, 1997, vol. 130, p. 433.
3. Rezaeivala, M. and Keypour, H., *Coord. Chem. Rev.*, 2014, vol. 280, p. 203.
4. Martell, A., Penitka, J., and Kong, D., *Coord. Chem. Rev.*, 2001, vol. 55, p. 216.
5. Brooker, S., *Eur. J. Inorg. Chem.*, 2002, p. 2535.
6. Guerriero, P., Tamburini, S., and Vigato, P.A., *Coord. Chem. Rev.*, 1995, vol. 139, p. 17.
7. Beer, P.D. and Smith, D.K., in: *Progress in Inorganic Chemistry*, Karlin, K.D., Ed., New York: Wiley, 1997, vol. 46, p. 1.
8. McKee, V., in: *Advances in Inorganic Chemistry*, Sikes A.G., Ed., S. Diego: Academic, 1993, vol. 40, p. 323.
9. Franken, A., Kilner, C.A., and Kennedy, J.D., *Inorg. Chem. Commun.*, 2003, vol. 6, p. 1104.
10. Vicente, J., Chicote, M.T., Martinez-Martinez, A.J., et al., *Org. Biomol. Chem.*, 2011, vol. 9, p. 2279.
11. Pepe, G., Cole, J.M., Waddell, P.G., and Perry, J.I., *Mol. Syst. Des. Eng.*, 2016, vol. 1, p. 416.
12. Dulong, F., Thuery, P., Ephritikhine, M., and Cantat, T., *Organometallics*, 2013, vol. 32, p. 1328.
13. Ferguson, G., Marsh, W.C., Lioyd, D., and Marshall, D.R., *Perkin Trans. 2 (1972–1979)*, 1980, p. 74.
14. Keypour, H., Rezaeivala, M., Valencia, L., and Perez-Lourido, P., *Polyhedron*, 2009, vol. 28, p. 4096.
15. Golbedaghi, R., Rezaeivala, M., and Albeheshti, L., *J. Mol. Struct.*, 2014, vol. 1076, p. 673.
16. Rezaeivala, M., Keypour, H., Salehzadeh, S., et al., *J. Iran Chem. Soc.*, 2014, vol. 11, p. 431.
17. Rezaeivala, M., Golbedghi, R., and Khalili, M., *Russ. J. Coord. Chem.*, 2016, vol. 42, p. 66. doi 10.1134/S1070328415120064
18. Golbedaghi, R., Rezaeivala, M., Khalili, M., et al., *J. Mol. Struct.*, 2016, vol. 1125, p. 144.
19. Kose, R., Gungor, S.A., Kariper, S.E., et al., *Inorg. Chim. Acta*, 2017, vol. 462, p. 130.
20. Karakas, D., *Turkish Comput. Theor. Chem.*, 2017, vol. 1, p. 1.
21. Sayin, K. and Karakas, D., *Spectrochim. Acta, Part A*, 2017, vol. 188, p. 537.
22. *International Tables for X-ray Crystallography*, Birmingham: Kynoch, 1952.
23. SAINT, Version 6.02, Madison: Bruker AXS, 1999.
24. Sheldrick, G.M., SADABS, Empirical Absorption Correction Program, Göttingen: Univ. of Göttingen, 1997.
25. XPREP, Version 5.1, Madison: Siemens Industrial Automation Inc., 1995.
26. Sheldrick, G.M., SHELXTL Reference Manual, Version 5.1, Madison: Bruker AXS, 1997.
27. Sheldrick, G.M., SHELXL-97, Program for Crystal Structure Refinement, Göttingen: Univ. of Göttingen, 1997.
28. Gauss View, Version 5, Semichem Inc., Shawnee Mission, KS, 2009.
29. *Gaussian 09, Revision C.01*, Frisch, M.J., Trucks, G.W., Schlegel, H.B., et al., Wallingford: Gaussian, Inc., 2009.
30. Perkin Elmer, ChemBioDraw Ultra Version (13.0.0.3015), Waltham: Cambridge Soft, 2012.
31. Becke, A.D., *J. Chem. Phys.*, 1993, vol. 98, p. 5648.
32. Lee, C., Yang, W., and Parr, R.G., *Phys. Rev. B: Condens. Matter. Mater. Phys.*, 1988, vol. 37, p. 785.
33. Keypour, H., Arzhangi, P., Rahpeyma, N., et al., *Inorg. Chim. Acta*, 2011, vol. 367, p. 9.
34. Hataway, A.J. and Underhill, D.E., *J. Chem. Soc.*, 1961, p. 3091.
35. Rosenthal, M.F., *J. Chem. Educ.*, 1973, vol. 50, p. 331.
36. Baver, A., Kirby, W.M.M., Sherris, J.E., and Turck, M., *Am. J. Clin. Pathol.*, 1986, vol. 45, p. 493.
37. Indu, M.N., Hatha, A.A.M., Abirosh, C., et al., *Braz. J. Microbiol.*, 1986, vol. 37, p. 153.